Design under uncertainty of solar hot water systems for hospitals

Antonio Atienza-Márquez, *Fernando* Domínguez Muñoz, *Francisco* Fernández Hernández, *José Manuel* Cejudo López

Energy Research Group (GEUMA), Department of mechanical, thermal and Fluids Engineering, Universidad de Málaga. C/Doctor Pedro Ortiz Ramos s/n, 29013 Málaga, Spain. E-mail: atienza-marquez@uma.es

Abstract. Failed designs are often behind underperforming solar hot water systems and excessive fossil fuel consumption in backup units. This paper proposed a reliable and robust method to design a solar thermal system combined with boilers for hot water preparation in a medium size-hospital hospital building with an average daily demand of 8.69 m^3. To start with, the conventional deterministic design, which assumes business-as-usual parameter values and overlooks their uncertainties, gives a required solar caption area of 223.0 m^2 to achieve an annual solar fraction of 70%. However, if the uncertainties of input parameters are considered, the reliability of this design solution is barely 22% regarding the solar fraction target set, and a solar caption area of 326 m^2 would be required to achieve a reliability of 90%. This work proposes a revised design solution which such high level of trustworthiness but with a lower solar caption area and, therefore, more attractive from an economic perspective. The strategy consists of narrowing the uncertainty bounds of those controllable parameters causing major variance on the system performance. A sensitivity analysis showed that the most significant uncertainties concerning the variance of the solar fraction are the following (in decreasing order of importance): variation of the hot water supplying set-point, insulation defects in the hot water distribution loop, wrong adjustment of thermostatic valves and dust deposition on collectors. According to the improved design proposed rooted in the revision of uncertainties through the installation of high-quality measurement and control equipment and effective maintenance, a design with a solar caption area of 257.3 m^2 would be enough to reduce the probability of failure below 10%.

Keywords. Domestic hot water, uncertainty, hospital building, solar thermal system, robust design.
DOI: https://doi.org/10.34641/clima.2022.161

1. Introduction

The integration of solar thermal systems in hospitals is a widespread solution to mitigate the carbon footprint of domestic hot water (DHW) production systems. Indeed, the minimum solar contribution required in such kind of large hot water consumer buildings is usually set from regulations, and thereby installations are designed accordingly.

In early design stages of these renewable energy systems, engineers use simulation programs that require various input parameters. However, these parameters are generally set with limited accuracy since they have a certain degree of tolerance. For instance, the random nature of the weather [1] or variables that depend on habits of users or the type of day, such as the hourly distribution of the hot water demand, are significant sources of uncertainty with a dramatic impact on the system performance.

The previous expertise on similar installations or the monitoring of key input data enhances the accuracy of simulation results, but uncertainties are never eradicated. The degradation of components (e.g., insulation materials) or modifications during the project execution are also significant sources of deviations between the expected system performance and the actual one. These factors can lead to weak designs with significant dependency on conventional backup systems like boilers. Numerous authors have applied uncertainty analysis to study the design of energy systems at buildings [2]. For instance, Ekström et al. [3] predicted the energy performance of a multi-family building using such kind of analysis. Li and Wang [4] proposed a robust design method for net-zero energy buildings using uncertainty analysis. A previous study [5] tackled the design under uncertainty of solar systems for hot water preparation in dwellings. Nevertheless, this issue is understudied in buildings with intensive domestic hot water demand such as hospitals.

This paper investigates a more robust and reliable design strategy of a solar thermal system for hot water preparation in hospital buildings. The reliability of the conventional design is evaluated through Monte Carlo stochastic simulations and then an improved design is proposed by narrowing the uncertainty bounds of those design parameters with major influence on the system performance.

2. Case-study hospital

2.1 Description and operation

Figure 1 shows the schematic layout of the DHW preparation system in a medium-size hospital, which is based on the "Hospital Comarcal de la Axarquía" with 193 beds and located Vélez-Málaga (36.75ºN, 4.09ºW), Spain. Basically, the installation is divided into (1) the solar thermal system, (2) the auxiliary system, and (3) the distribution network. The auxiliary system consists of gas-fired boilers and a pasteurizer that prevent legionella growth and supplies DHW at the specified set-point. Regarding the DHW distribution network, the system operation is continuous (i.e., 24 hours per day) with a constant recirculation flow rate. Therefore, there is always hot water available at the consumption points with low waiting times.

The system operates as follows. The water leaving the solar field (stream S1) flows through the hot side of heat exchanger HE-1, heating the cold water coming from the bottom of the stratified solar storage tank. The fluid leaving the hot side of the heat exchanger HE-1 is still at high temperature and is used in the heat exchanger HE-2 to preheat the incoming consumption water coming from the water reservoir. This preheated water leaving the heat exchanger HE-2 (stream W2) enters the service tank, where it is mixed with the recirculated flow (stream W7) and the water stream W3 that has absorbed the heat from the solar storage circuit through the heat exchanger HE-3. If the water temperature at the top of the service tank is below the supplying set-point, the water stream W5 enters the pasteurizer. As shown in Figure 2, this unit is fed with the hot water produced in the gas boilers. Afterward, the water stream W6 is distributed through the DHW pipeline network up to the consumption points distributed throughout the building.

The control system plays a key role in the energy management of the installation. The following control algorithm is applied to the different pumps of the system:

- Pump P1 (solar primary circuit) is activated when the radiation level on the caption plane is above a pre-set value or turned off if the radiation falls below a pre-fixed limit. Additionally, the controller of the pump P1 is equipped with an inverter to control proportionally the pumping capacity between 100% to 50% in function of the temperature of the stream S1.

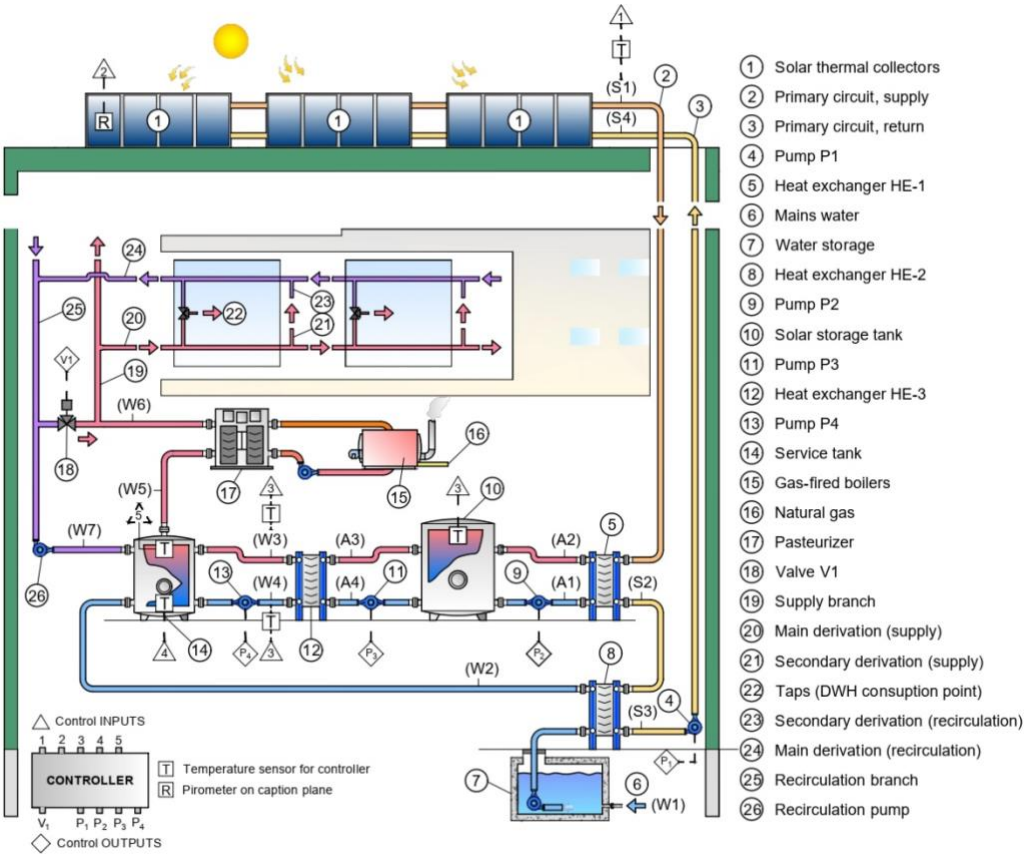

Fig. 1 – Schematic layout of the domestic hot water preparation system in the case-study hospital building.

- Pump P2 (solar storage, i.e., secondary circuit) is activated whether the temperature of the stream S1 leaving the solar collectors is a pre-set quantity higher than the temperature at the upper level of the solar storage tank. Pump P2 is a constant flow pump.

- Pump P3 (discharge of the solar storage tank) is activated when the temperature at the top of the solar storage tank is a pre-set quantity higher than the temperature at the bottom of the service tank.

- Pump P4 follows the same control logic as pump P3. Nonetheless, the inverter controller of pump P4 regulates proportionally the flow rate between 50% to 100% in function of the temperature difference between streams W3 and W4 (heat exchanger HE-3).

- Pump P5 (recirculation) is always activated.

The function of the thermostatic two-way valve V1 installed in the recirculation manifold is to avoid supplying temperatures above the DHW set point.

2.3 Mathematical modelling

The system was modelled using TRNSYS 18 [6]. The simulation time-step was set to 5 minutes. The global steady-state energy balance of the system (Figure 1) is written as follows:

$$Q_S + Q_P - D = 0 \quad (1)$$

where ΔU denotes the variation of internal energy in pipes (modelled with Type 31) and service tank (modelled with Type 158). Both the thermal losses through the primary circuit and the solar storage circuit are implicitly included in the solar production (Q_S) term, which is calculated from the energy balance in the heat exchangers HE-2 and HE-3 (modelled with Type 91):

$$Q_S = Q_{HE\text{-}2} + Q_{HE\text{-}3} = m_{W1} \times Cp \times (T_{W2} - T_{W1}) + m_{W3} \times Cp \times (T_{W3} - T_{W4}) \quad (2)$$

where m and Cp are the mass flow rate and specific heat of water streams, respectively. The solar collectors are modelled using TRNSYS Type 1. The net solar caption area of a single collector is 8.578 m^2 with a connection pattern of two in series.

The DHW demand (D, in kW) includes thermal losses throughout the distribution pipes and in the service tank and is calculated as follows:

$$D = m_{W1} \times Cp \times (T_{W6} - T_{W1}) + m_{W7} \times Cp \times (T_{W6} - T_{W7}) + Q_{L,\,\text{servicetank}} \quad (3)$$

The baseline monthly average temperatures of the tap water reservoir (T_{W1}) from January to December are the following (in ^{o}C): 16.5, 17.4, 18.0, 18.3, 20.2, 21.5, 22.7, 23.0, 21.9, 20.1, 18.8, 16.6. The hourly DHW demand (V_{DHW}, in L/h) is calculated as:

$$V_{DHW} = \Omega \times \alpha \times V_{av,DHW} \quad (4)$$

where $V_{av,DHW}$ is average daily DHW demand. On the other hand, the parameters α and Ω represent the DHW hourly demand ratio (Figure 2) and the baseline daily dimensionless demand (Figure 3, together with other two profiles that will be use in the uncertainty analysis), respectively. Both parameters have been developed from the statistical analysis of the data gathered from the monitoring of the hospital in which the case-study presented in this paper is based on.

The thermal energy supplied to the DHW stream in the pasteurizer (Q_P) is calculated as follows:

$$Q_P = m_{W5} \times Cp \times (T_{W6} - T_{W5}) \quad (5)$$

The total thermal losses through the DHW distribution pipelines (Q_L) are calculated as the sum of the thermal losses through each i-pipe section:

$$Q_L = \sum UA_i \times \Delta T_{m,1} \quad (6)$$

As shown in Table 1, the pipes are classified into these three categories: main branches, main derivations, and connections with taps.

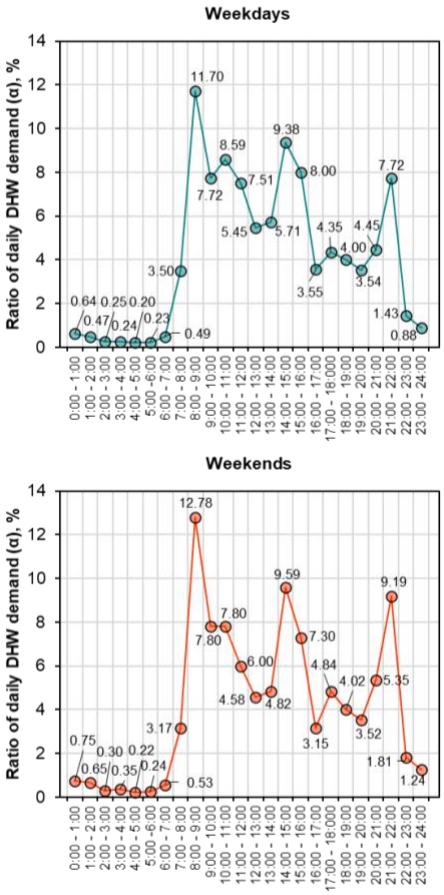

Fig. 2 – Hourly domestic hot water demand ratio for weekdays and weekends.

Tab. 1 – Number and dimensions (outer and inner diameters, length, and thermal insulation thickness) of the domestic hot water pipeline distribution categories [7,8]. Thermal conductivity of pipes and insulation: 0.24 and 0.04 W/(m·K).

Pipe	Supply					Recirculation				
	No.	o.d./i.d., mm	Ins., mm-thick	*U*-value, W/(m²·K)	Total length, m	No.	o.d./i.d., mm	Ins., mm-thick	*U*-value, W/(m²·K)	Total length, m
Branches	9	40.0/29.0	30	2.84	135.0	9	20.0/14.4	25	4.25	135.0
Main derivations	27	32/23.2	25	3.45	270.0	27	16.0/11.6	25	4.69	270.0
Connections with taps	135	20/14.4	25	4.25	337.5	135	16.0/11.6	25	3.09	337.5

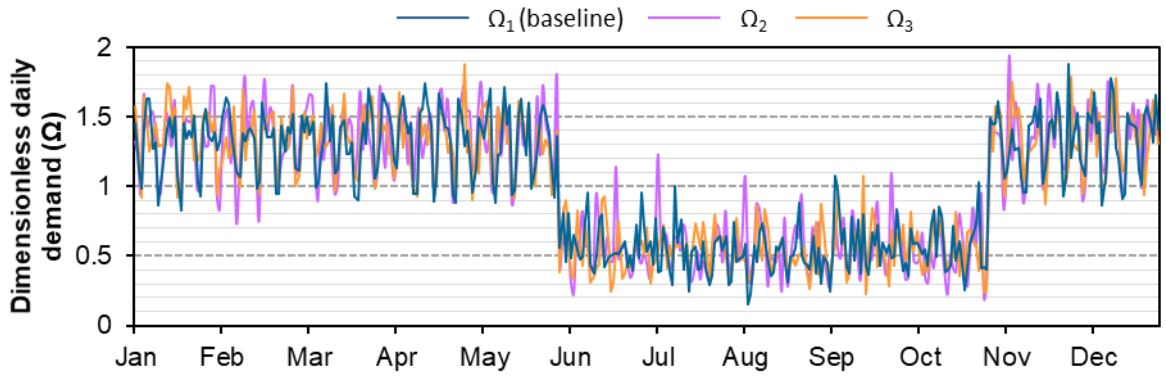

Fig. 3 – Baseline dimensionless daily domestic hot water demand.

The log-mean temperature difference of each pipe section (ΔT_m) is calculated from the following expression:

$$\Delta T_{m,i} = (\Delta T_{1,i} - \Delta T_{2,i})/\ln(\Delta T_{1,i} \times \Delta T_{2,i}^{-1}) \quad (7)$$

where $\Delta T_{1,i} = T_{W,in,i} - T_{amb}$, and $\Delta T_{2,i} = T_{W,out,i} - T_{amb}$. The term T_{amb} is the temperature of the surrounding air, and it is assumed that the whole DHW distribution pipeline layout is inside the building. The overall heat transfer coefficient for each pipeline category (UA_i) is approximated as follows:

$$1/UA_i = \ln[(d_{o,i} + 2\times\delta_i)/d_{o,i}] \times (2\,\pi\,k\,L_i)^{-1} \quad (8)$$

where d_o, k and δ represent the outer pipe diameters and thermal conductivity and thickness of the insulation material, respectively. The parameter L is the total length of each pipeline type. Note that the same strategy is followed to calculate the thermal losses through the primary circuit pipelines and through both the solar and service tank, whose baseline insulation thickness is estimated accordingly with the Spanish standard for thermal systems at buildings [7].

The annual solar fraction (SF) and utilization factor (UF) of the system is defined as follows:

$$SF = \int Q_S \cdot \mathrm{d}t \,/\, \int D \cdot \mathrm{d}t \times 100\% \quad (9)$$

$$UF = \int Q_S \cdot \mathrm{d}t \,/\, \int A \cdot I_T \cdot \mathrm{d}t \times 100\% \quad (10)$$

where A is the net caption area of the solar installation and I_T is the solar radiation on the caption plane.

2.3 Identification and quantification of uncertainties

Table 2 depicts the base-case values and the distributions proposed to model the uncertainties of the input parameters involved in the design of the system. The column "base values" contains a reasonable combination of inputs that any designer could have chosen to solve the problem in a deterministic fashion. The column "distributions" defines the probability density function associated with each factor. These distributions have been proposed based on literature recommendations, theoretical considerations or educated guesses [5].

The Monte Carlo method is used to propagate the uncertainty of the different input parameters given in Table 2 and generate a sample of 1,500 simulations. Finally, the reliability (R) of the deterministic design is calculated from the following expression:

$$R = N_{feasible}/N_{runs} \times 100\% \quad (11)$$

where $N_{feasible}$ is the number of simulation runs that achieved the minimum solar fraction of 70%, and N_{runs} is the total number of simulation runs conducted.

Tab. 2 – Baseline values and uncertainty range of the input parameters of the environment. Sources: [5,8,9].

Factor X	Description	Base values	Distribution
1	Hourly weather data: Total horizontal radiation ($G_{t,i}$), kWh/m^2, and outdoor ambient temperature ($T_{o,i}$), ^{o}C.	Contemporary	UD [Contemporary, RCP2.6, RCP4.5, RCP8.5]
2	Monthly average mains water temperature, ^{o}C.	$T_{W1,i}$	$T_{W1,i}$ + U [0, 3]
3	Tilted surface radiation model.	Isotropic	UD [Isotropic, Hay, Reindl, Perez]
4	Angular height of remote obstacles, deg (^{o})	10	UD [8, 12]
5	Ground reflectivity.	0.25	U [0.15, 0.55]
6	Dusting effect on collector transmissivity.	1	U [0.9, 1]
7	Weighting factor (*wf*) between outdoor ambient (T_o) and temperature of conditioned zones (T_r, interior spaces such as wall cavities or plenums inside where pipes run through): $T_{amb} = wf \times T_o + (1-wf) \times T_r$	0.5	U [0.2, 0.8]
8	Weighting factor between outdoor ambient and temperature of conditioned zones (basement): $T_{amb,\ basement} = wf \times T_o + (1-wf) \times T_{r,\ basement}$	0.8	U [0.3, 0.9]
9	Average daily DHW demand ($V_{av,DHW}$), m^3/day.	8.66	$V_{av,DHW}$ × U [-0.8, 1.2]
10	Daily dimensionless DHW demand (Ω).	Ω_1	UD [$\Omega_{1...3}$] (Fig. 3)
11	Hourly ratio of daily DHW demand (α).	α	- (Fig. 2)
12	No. of solar collectors.	N_c	-
13	Collectors' slope, deg (^{o}).	45	-
14	Collectors' azimuth, deg (^{o}).	0	-
15	Intercept collector efficiency at normal incidence, $F_R(\tau\alpha)_n$.	0.795	N [0.795, 0.00494]
16	Slope of collector efficiency ($F_R U_L$), W/(m^2·K).	4.177	N [4.177, 0.11934]
17	First order incidence angle modifier.	0.14	N [0.14, 0.0014]
18	Flow rate through each solar collector, L/(h·m^2).	70	LN [70, 35; 30, 210]
19	Ethylene-glycol concentration (primary circuit), %.	20	U [0, 30]
20	Effectiveness of heat exchangers (ε).	0.82	U [0.60,0.82]
21	*U*-value of the primary circuit pipes, based on the inside pipe surface area, W/(m^2·K).	1.83	1.83 × T [1.0, 2.0, 1.0]
22	Total length of primary circuit pipelines, m.	50	30×U [0.9 1.1]
23	Storage volume of the solar tank, L/m^2.	75	-
24	*U*-value of the solar tank, based on the inside surface area, W/(m^2·K).	0.50	0.50 × T [1.0, 2.0, 1.0]
25	Pump P2 flow rate (V_{P2}), L/h.	V_{P1}	V_{P1}×N [1,0.20]
26	Pump P3 flow rate (V_{P3}), L/h.	V_{P1}	V_{P1}×N [1,0.20]
27	Pump P4 flow rate (V_{P4}), L/h.	V_{P1}	V_{P1}×N [1,0.20]
28	*U*-value of the service tank, based on the inside surface area, W/(m^2·K).	0.50	0.50 × T [1.0, 2.0, 1.0]
29	Storage volume of the service tank, L/m^2.	40	-
30	Total length of distribution pipelines ($L_{tot,\ design}$), m.	$L_{tot,\ design}$	$L_{tot,\ design}$ × U [0.9, 1.1]
31	*U*-value of DHW pipes (supply and recirculation), based on the inside pipe surface area, W/(m^2·K).	*U*-value (Tab. 1)	*U*-value × T [1.0, 2.0, 1.0]
32	Recirculation flow rate (V_{rec}), L/h.	V_{rec} = max (250×No. branches, Q_L/3.48)	V_{rec} × N [1, 0.20]

Tab. 2 (cont.) – Baseline values and uncertainty range of the input parameters of the environment. Sources: [5,8,9].

Factor X	Description	Base values	Distribution
33	DHW supply set-point temperature ($T_{sp,DHW}$), ºC.	60	T [55,65,60]
34	Maximum solar tank temperature, ºC.	90	T [88, 90, 92]
35	Maximum service tank temperature, ºC.	90	T [88, 90, 92]
36	Radiation level for activation of Pump P1, W/m^2.	185	T [185, 190, 180]
37	Lower radiation limit to keep pump P1 switched on, W/m^2.	160	T [160, 165, 155]
38	Pump P1's frequency shifter temperature set-point (T_{S1}) for 100% capacity, ºC.	85	U [80, 90]
39	Pump P1's frequency shifter temperature set-point (T_{S1}) for 50% capacity, ºC.	15	U [10, 20]
40	Upper ΔT (T_{S1}-T_{A3}) to switch on pump P2, ºC.	1.5	T [1.0, 2.0, 1.5]
41	Lower ΔT (T_{S1}-T_{A3}) to switch off pump P2, ºC.	0.5	T [0.0, 1.0, 0.5]
42	Upper ΔT (T_{A3}-T_{A4}) to switch on Pumps P3 and P4, ºC.	5.0	T [3.0, 7.0, 5.0]
43	Lower ΔT (T_{A3}-T_{A4}) to switch off Pumps P3 and P4, ºC.	1.0	T [0.0, 2.0, 1.0]
44	Upper ΔT (T_{W3}-T_{W4}) to set the frequency shifter of P4 at 50 Hz (i.e., 100% of its pumping capacity), ºC.	5.0	U [4.0, 6.0]
45	Lower ΔT (T_{W3}-T_{W4}) to set the frequency shifter of P4 at 25 Hz (i.e., 50% of its pumping capacity), ºC.	1.0	U [0.0, 2.0]
46	Adjustment of valve V1 concerning the hot water supply set-point temperature (factor X-33).	1.0	N [1,0.05]

Nomenclature of distributions. U [a, b]: Uniform distribution between a and b; UD [a, b]: Uniform discrete distribution between a and b; LN [λ, ξ; a, b]: Truncated lognormal with mean value λ, and standard deviation ξ truncated between a and b; T [a, b, c]: Triangular distribution with minimum value a, maximum value b and likeliest value c; N [μ, σ]: Normal is a normal distribution with mean value μ and standard deviation σ.

3. Results and discussion

2.1 Reliability of the deterministic design

Table 3 shows the deterministic or base results obtained running the TRNSYS model for different caption areas (i.e., ranging between 32 to 52 solar collectors) using the baseline parameters given in Table 2. The reliability of achieving a minimum solar fraction of 70% (required by the Spanish energy code for buildings for the specified location and its corresponding climatic zone [10]) is also provided for each design-case.

According to the deterministic results, which overlooks the uncertainty of the different input parameters involved in the design, a solution with 26 solar collectors (i.e., net caption area of 223.0 m^2) would be required. In such case, the solar fraction and utilization factors calculated are 70.7% and 41.7%, respectively. However, the Monte Carlo results depicted in Figure 4 show that the possible outcomes of the model spread across a large region when it is considered the effect of the uncertainties on this deterministic solution. In fact, the reliability of the deterministic design barely achieves 22%. Therefore, deviations in operating conditions and system characteristics could lead into a failed design, so the solar fraction of the installation once executed is likely to underperform concerning the target.

2.2 Design improvement

The trivial solution to enhance the reliability of the system consists solely of oversizing the solar field. As shown in Table 3, a design solution with 38 solar collectors (326.0 m^2) would achieve the minimum annual solar fraction with a reliability beyond 90%. Nevertheless, this solution is far from ideal because a huge capital investment would be required. Besides, the system will more likely suffer from long harmful stagnation periods in the summertime [5].

An effective strategy to improve the reliability of the design is based on identifying those sources of uncertainty with major impact on the system performance through a sensitivity analysis. Afterwards, the objective will be focused on narrowing the allowed range of variation of these parameters, but only whether they are somehow controllable.

Tab. 3 – Solar fraction, utilization factor and reliability of the design for different number of solar collectors considered.

No. of solar collectors	Net caption area, m²	*SF*, %	*UF*, %	Design reliability, %
24	205.9	67.6	43.0	9.7
26	223.0	70.7	41.7	22.4
28	240.2	73.6	40.4	36.9
30	257.3	76.3	39.2	46.7
32	274.5	78.8	38.1	60.9
34	291.7	81.1	37.1	74.1
36	308.8	83.3	36.1	83.3
38	326.0	85.2	35.1	90.0

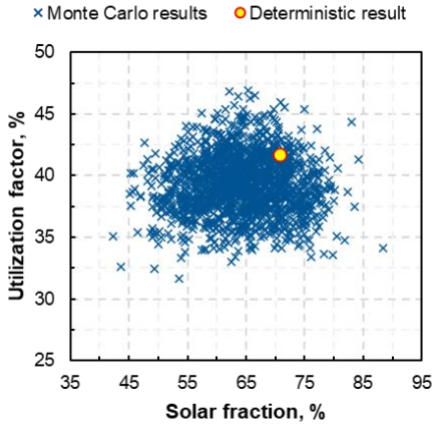

Fig. 4 – Solar fraction and utilization factor of the deterministic design (26 collectors, 223.0 m²).

Figure 5 shows the Standardized Regression Coefficients (SRCs) obtained from the sensitivity analysis using Monte Carlo sampling. The numbering of the design parameters corresponds to the given in Table 2. Since the system modelling varies linearly and is additive (R-square 0.95), the SRC coefficients obtained can be considered meaningfulness. The sign of these coefficients indicates if the output increases (positive) or decreases (negative) as the corresponding input factor increases. According to the results obtained, the following design parameters explains most of the variance of the solar fraction reported by the modelling:

1. *U*-value of the DHW distribution pipes (factor X-31, SCR = -0.54).

2. Hot water supply set-point temperature (factor X-33, SRC = -0.49).

3. Deviation of valve V1 (factor X-46, SCR = -0.31).

4. Average daily demand (factor X-9, SCR=-0.30).

5. Dust on solar collectors (factor X-6, SRC = 0.28).

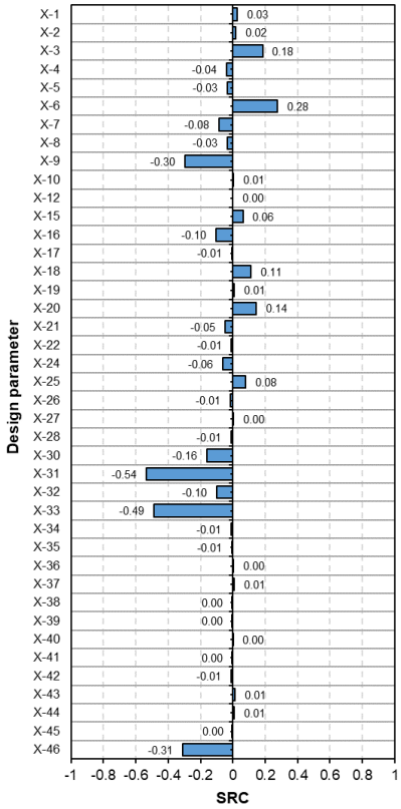

Fig. 5 – Standardized sensitivity coefficients for each input parameter involved in the design (Table 2).

An effective thermal insulation of hot water pipes is central to avoid excessive thermal losses along lengthy DHW distribution networks of medium/large buildings. Regarding the DHW supplying set-point temperature and wrong adjustment of the valve V1, higher temperatures require higher natural gas consumption (because boilers must switch on more often) and involves higher thermal losses both through the distribution pipelines and in the service tank. Consequently, the lower is the hot water supplying temperature, the higher solar fraction for a given caption area. Nevertheless, the temperature of the hot water at taps and through recirculation loops must be above 50ºC due legionella issues. Thus, because of thermal losses through the distribution circuit, there is little chance to supplying the hot water below 60ºC. Nonetheless, the uncertainty ranges around the set-point can be narrowed, for example, by installing top quality valves and measurement and control devices.

On the other hand, an effective maintenance of the system is crucial to avoid the worsening of the solar fraction because of dust deposition on collectors or concerning the early detection of insulation defects that set off thermal losses. However, there are parameters with a significant impact of the performance of the system but whose uncertainty are uncontrollable, for example, the average daily domestic hot water demand.

But regarding an improved design, what should be the *target reliability*? Ultimately, this is a decision for

the engineer designing the system. In this paper, the authors assume a minimum target of 90%. As an example, it is proposed an improved design with the following revised uncertainties: deviation of the baseline *U*-value of the DHW distribution pipes (factor X-31) T [1.0, 2.0, 1.0]; hot water supplying set point (factor X-33) T[58, 62, 60]; deviation of thermostatic valve V1 (factor X-46) N[1, 0.01]; and dusting effect on collector transmissivity (factor X-6) U[0.98, 1]. The rest of uncertainty distributions remains as given in Table 2. Figure 6 shows the Monte Carlo simulation results for this revised and improved design and for the case of 30 solar collectors installed. As a result, the reliability fairly enhances concerning the original design for such number of collectors (i.e., from 70.7% to 90.3%).

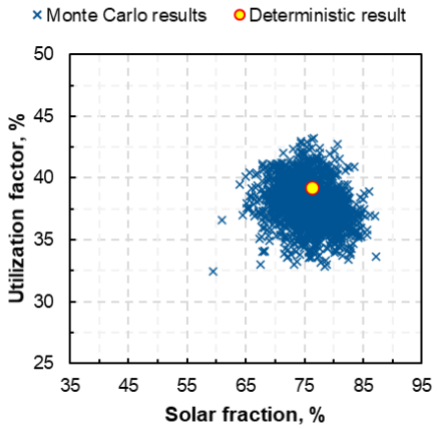

Fig. 6 – Solar fraction and utilization factor of the revised design (30 collectors installed, 257.3 m^2).

4. Conclusions

In this paper, the authors explored the improved design of a solar thermal system for domestic hot water preparation in a medium-size hospital.

It was found that the uncertainty of the following factors introduced a dramatic variance of the solar fraction: the hot water supplying set-point, lack or defect in thermal insulations, wrong adjustment of valves, as well as factors requiring an intensive maintenance such as the periodic cleaning of solar collectors. While the reliability of the original design (22%) which overlooks the uncertainty of input parameters could be enhanced up to 90% just by expanding the solar field from 26 to 38 solar collectors (i.e., from 223.0 to 326.0 m^2), the revised design proposed in this paper requires only 30 solar collectors (257.3 m^2). The strategy followed is more attractive from an economic perspective and it was rooted in narrowing the uncertainties of those controllable input parameters with major impact on the system performance. Despite a lacking fixed rule to reduce the uncertainty of design parameters beyond expertise, the use of high-quality measurement and control equipment as well as an effective maintenance are both vital to reduce the probability of failed designs down to acceptable risks.

In a future work, the authors will study the trade-off between increasing the reliability of the design of the energy system presented in this paper and its economic performance throughout its lifetime.

5. Acknowledgement

The authors acknowledge the Universidad de Málaga and "*Programa Operativo FEDER Andalucía 2014-2020*" the financial support of the contract UMA18-FEDERJA-247, and Mr. Pedro Quintero Jiménez for providing data and helpful information.

6. References

[1] Lan B., Tian Z., Wu X. A simplified method of generating sequential meteorological parameters for uncertainty-based energy system design, Energy Build, 2021;237:110780.

[2] Mavromatidis G., Orehounig K., Carmeliet J. A review of uncertainty characterisation approaches for the optimal design of distributed energy systems, Renew Sustain Energy Rev, 2018;88:258–277.

[3] Ekström T., Burke S., Wiktorsson M., Hassanie S., Harderup L.E., Arfvidsson J. Evaluating the impact of data quality on the accuracy of the predicted energy performance for a fixed building design using probabilistic energy performance simulations and uncertainty analysis, Energy Build, 2021;249:111205.

[4] Li H., Wang S. Coordinated robust optimal design of building envelope and energy systems for zero/low energy buildings considering uncertainties, Energy Build, 2020;265:114779.

[5] Domínguez-Muñoz F., Cejudo J.M., Carrillo-Andrés A., Ruivo C.R. Design of solar thermal systems under uncertainty, Energy Build, 2012;47: 474–484.

[6] TRNSYS 18, https://sel.me.wisc.edu/trnsys/features/features.html (Accessed 13/01/2022).

[7] Reglamento de Instalaciones Térmicas en los edificios (RITE), 2013.

[8] Documento Básico HS-4 Suministro de agua, https://www.codigotecnico.org/pdf/Documentos/HS/DBHS.pdf (Accessed 12/01/2022).

[9] Meteonorm (2021). https://meteonorm.com (Accessed 13/01/2022).

[10] Código Técnico de la Edificación, Sección HE-4: Contribución solar mínima de agua caliente sanitaria.